

Electrostatic Protein–Chromophore Interactions Promote the *all-trans* → 13-*cis* Isomerization of the Protonated Retinal Schiff Base in Bacteriorhodopsin: An *ab Initio* CASSCF/MRCI Study

Marco Nonella*

Lehrstuhl für BioMolekulare Optik, Ludwig-Maximilians-Universität München, Oettingenstrasse 67, D-80538 München, Germany

Received: May 24, 2000; In Final Form: August 24, 2000

Ab initio calculations of the potential energy surfaces of the states S_0 , S_1 , and S_2 of protonated Schiff base model molecules containing three, four, and five conjugated double bonds have been carried out at the HF/MRCI and CASSCF/MRCI levels of theory. Our calculations demonstrate that predictions of crossings of electronic states depend on the method of calculation and are different at the CASSCF and CASSCF/MRCI levels. Moreover, when a counterion is added in the vicinity of a protonated Schiff base, HF/MRCI and CASSCF/MRCI calculations predict different regions for S_0/S_1 crossing. The length of the conjugated system seems not to affect such qualitative results considerably. Our calculations suggest that (i) the second excited state is of no importance for the primary step of the photocycle of bacteriorhodopsin, (ii) an efficient decay into the electronic ground state during an *all-trans* → 13-*cis* isomerization is only possible due to the interaction of the protonated Schiff base with a counterion, (iii) this isomerization reaction can occur spontaneously only after a preceding relaxation of bond lengths in the excited state, and (iv) an *all-trans* → 13,14-di-*cis* double isomerization is most likely inefficient due to a nonvanishing barrier in the excited state.

1. Introduction

The structure and function of bacteriorhodopsin has been the topic of many experimental and theoretical investigations; recent reviews can be found in refs 1 and 2. In short, a catalytic cycle is induced after light excitation of the protein's chromophore. This chromophore is a retinal molecule which is covalently bound to Lys-216, forming a protonated Schiff base. During the photocycle, the chromophore changes its conformation and its protonation state such that one proton per absorbed photon is pumped across the membrane. The mechanism of the very fast primary reaction of bacteriorhodopsin is still not known in detail. One of the unresolved problems concerns the reaction coordinate for the fast *all-trans* → 13-*cis* isomerization. One model assumes a single isomerization around the $C_{13}=C_{14}$ double bond τ_{13} ,³ while a second model suggests a double isomerization around the $C_{13}=C_{14}$ double bond τ_{13} and around the adjacent $C_{14}=C_{15}$ single bond τ_{14} ,^{4–6} resulting in a perturbed 13,14-di-*cis* conformation. A second unresolved problem concerns the question whether the isomerization reactions can be discussed using a two-state model by considering only the electronic states S_0 and S_1 or in how far consideration of the second excited state S_2 might be necessary. A two-state model was proposed on the basis of stimulated emission experiments.^{7,8} More recent time-resolved absorbance measurements,^{9,10} however, are in better agreement with a three-state model. On the theoretical side, *ab initio* calculations on model molecules at the CASSCF,^{11,12} CASSCF/PT2,¹³ and HF/MRCI¹⁴ levels of theory gave no evidence for a crossing of states S_1 and S_2 , while CASSCF calculations by Schulten and co-workers^{15,16} predicted such a crossing for an *all-trans* → 13-*cis* single isomerization.

The 11-*cis* → *all-trans* isomerization reaction, which corresponds to the primary process occurring in rhodopsin,^{17–19} has recently been studied by means of a newly developed density functional method.²⁰ The method allows structural relaxation and molecular dynamics in the first excited singlet state under the assumption of a single HOMO–LUMO excitation.²¹ A significant barrier has been found for this process which clearly disagrees with experimental data. However, inclusion of a counterionic group and a water molecule reduced this barrier in the excited state by 10 kcal/mol. Although the findings of this study suggest that the chosen method is not really appropriate for investigating this system, it nevertheless emphasizes the importance of including chromophore–protein interactions in theoretical studies in order to gain a deeper insight into the mechanism of this isomerization reaction.

The isomerization reactions *all-trans* → 13-*cis* and *all-trans* → 11-*cis* of the complete protonated Schiff base of retinal and of a model molecule consisting of six conjugated double bonds have recently also been studied by means of state-averaged CASSCF methods.^{22,23} In these calculations, however, a rather limited active space generated by distributing 6 electrons among 5 active orbitals was applied. For the *all-trans* → 13-*cis* reaction, a small barrier was found in the excited state around 130°.²² This barrier was not significantly affected upon addition of a counterion or a water molecule in the vicinity of the $-NH^+$ group. The counterion, however, reduced the energy difference between the states S_0 and S_1 considerably. A very similar behavior was also found for the isomerization reaction *all-trans* → 11-*cis*.²³

Recent experiments with $C_{13}=C_{14}$ locked retinal analogues^{24,25} have shown that the experimentally detected very fast primary process is most likely not connected to a rotational isomerization reaction but to a relaxation of bond lengths after

* To whom correspondence should be addressed. E-mail: nonella@physik.uni-muenchen.de.

excitation of the chromophore into the first excited state. These findings are in agreement with the results of minimum-energy path calculations on potential energy surfaces of protonated Schiff base model molecules of Garavelli et al.^{11,12} According to these calculations a very fast relaxation of bond lengths precedes a torsional motion around the C=C double bond which corresponds to the C₁₃=C₁₄ double bond of the protonated retinal Schiff base. During this rotation a conical intersection between the states S₀ and S₁ is reached which makes an efficient relaxation into the electronic ground state possible. Similarly, a crossing of the ground state and first excited state has been found by Schulten and co-workers^{15,16} for a slightly different molecular system consisting of four conjugated double bonds.

In our own calculations on a small protonated Schiff base model molecule, we have applied a HF/MRCI method.¹⁴ This method did not allow us to consider structural relaxation during the calculation of energy profiles for isomerization reactions. We were therefore not able to search for conical intersections and have based the discussion of our results on the analysis of the character of the CI wave functions. We have found an S₀/S₁ crossing only along the coordinate of a double isomerization around the central double bond (corresponding to C₁₃=C₁₄ in retinal) and the adjacent single bond (corresponding to C₁₄=C₁₅ in retinal) and have concluded that only this reaction can provide an efficient decay into the electronic ground state.

While we had applied a HF/MRCI approach, other studies have usually chosen state-averaged CASSCF methods. Although CASSCF methods are very efficient for the calculation of excited states, they often suffer from convergence problems. To avoid such problems, state-averaging methods are usually applied in such calculations. We had in our previous work decided to use multireference CI methods in order to avoid possible artifacts caused by the state-averaging procedure. As reference for our MRCI calculations we have used the Hartree–Fock wave function of the electronic ground state. The quality of this reference function might, however, be too poor to provide physically correct results.

The contradictory results provided by different quantum chemical methods seriously affect the discussion of the fast primary step of bacteriorhodopsin's photocycle. Further investigations of this topic are thus inevitable in order to provide useful contributions from the theoretical side.

In this study, we have continued our studies on the small model system we have used in our previous contribution.¹⁴ We have again carried out multireference CI calculations but this time by using a reference wave function generated by a state-averaged CASSCF calculation which is very similar to the calculation carried out by Garavelli et al. Our calculations show that an S₀/S₁ crossing upon a single rotation around the C=C double bond is found at the CASSCF level. With our method of calculation, we cannot decide whether this crossing corresponds to an avoided or real crossing of electronic states. From comparison with the results of Garavelli et al., however, we conclude that the state crossing found in our calculations must most likely correspond to their conical intersection. Interestingly, this state crossing is lost after the following MRCI calculation.

We use then equivalent methods for calculations on a model molecule which closely corresponds to the molecule used by Schulten et al. in their studies. We essentially find the same results as we have found for the small system with three conjugated double bonds. For this larger molecule, we have also modeled a simple Schiff base—counterion system by placing a negative unit charge in the vicinity of the —NH⁺ group to check for the effect of protein—chromophore interactions. We find

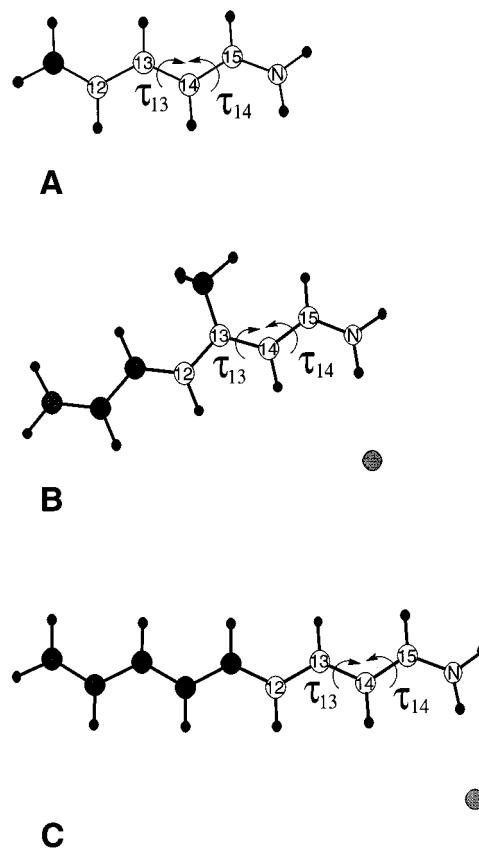


Figure 1. Structures of the Schiff base model molecules used in this study.

that protein—chromophore interactions cause a crossing between ground and excited states also along the reaction coordinate of the single isomerization.

We finally present the results of HF/MRCI and CASSCF/MRCI calculations on a system with five conjugated double bonds. As long as no interaction of the protonated Schiff base with a counterion is taken into account, the results of the two methods of calculation are qualitatively in good agreement. As soon as a counterion is added to the system, the CASSCF/MRCI method predicts a crossing of the states S₀ and S₁ along both reaction coordinates, while with the simpler HF/MRCI method such a crossing is only predicted during a simultaneous rotation around single and double bonds.

2. Computational Details

SCF, CASSCF, and MRCI calculations have been carried out with version 5.5 of the COLUMBUS^{26,27} package of programs which uses routines taken from the program DALTON.²⁸ The basis sets used in most of the presented calculations are the 6-31G and 6-31G* basis sets of Pople and co-workers.^{29–31} The quality of the chosen basis set is limited by the prohibitively fast growing size of MRCI calculations of the chosen model molecules.

For the molecule with three conjugated double bonds (molecule A in Figure 1), we have carried out two sets of calculations. The first set of calculations was using the 6-31G basis set. In the CASSCF step, all excitations within an active space consisting of 6 orbitals and 6 electrons were considered. The states S₀, S₁, and S₂ were included in the state-averaged CASSCF calculation.

For the MRCI calculation, the 6 core orbitals and 14 virtual orbitals were frozen. The reference space was defined by all

possible single and double excitations from the two highest occupied orbitals into the two lowest virtual orbitals. This method leads to 15 reference configurations and 3.6 millions of configuration state functions (CSFs). Inspection of the results ensured that all configurations which show an expansion coefficient larger than 0.1 in the optimized CI wave functions are contained in the reference configurations. In the second set of calculations, we applied the 6-31G* basis set, since polarization functions might be essential for a proper description of this system. The same basis set has also been used in the calculations of Garavelli et al. The reference wave function for the MRCI calculations has again been generated in a CASSCF calculation using 6 electrons and 6 orbitals. In the CI step, the 6 core orbitals and 28 virtual orbitals (all orbitals with orbital energies higher than 1.5 au) were frozen. Again, all single and double excitations from the two highest occupied orbitals into the two lowest virtual orbitals were considered as reference configurations. This setup results in nearly 8 million CSFs.

For the molecule with four conjugated double bonds (molecule **B** in Figure 1) we have chosen a similar approach. As basis set the 6-31G standard basis was applied. Our reference wave function was generated with a state-averaged CASSCF calculation using 6 electrons and 6 orbitals (CASSCF(6,6)). The states S_0 , S_1 , and S_2 were included in the state-averaged CASSCF calculation. The reference space for the MRCI calculation consisted of 10 configurations which were selected according to their contribution to the CI wave function on selected points equally distributed on the potential energy surface. These 10 configurations are described as: $(32)^2 (33)^2$ (HF determinant), $(32)^2 (33)^1 (34)^1$, $(32)^2 (33)^1 (35)^1$, $(32)^2 (34)^2$, $(32)^2 (34)^1 (35)^1$, $(32)^1 (33)^2 (34)^1$, $(32)^1 (33)^2 (35)^1$, $(32)^1 (33)^1 (34)^2$, and two combinations of $(32)^1 (33)^1 (34)^1 (35)^1$. 20 occupied and 30 virtual orbitals were frozen in the CI calculations. This setup resulted in 2.7 million CSFs.

The calculations on the system with five conjugated double bonds (structure **C** in Figure 1) have also been carried out using the 6-31G standard basis set. For this molecule we have carried out HF/MRCI and CASSCF/MRCI calculations. 20 core and 30 virtual orbitals of a total of 114 molecular orbitals have been frozen in the CI calculation. The active space of the CASSCF calculation was generated using 6 electrons and 6 orbitals, corresponding to a CASSCF(6,6) calculation. Again the three lowest electronic states were included in the state-averaged CASSCF procedure. The reference configurations for the MRCI calculations were the same in both methods and had been selected by carrying out SRCI calculations on all considered points of the potential energy surface. According to these calculations, the two highest occupied orbitals and three lowest unoccupied orbitals were contained in the reference space for the MRCI calculations. Within this active space, single and double excitations were allowed with the restriction that only single excitations were allowed from the second highest occupied orbital and into the third lowest unoccupied orbital. This setup leads to 20 reference configurations and about 5.3 million CSFs. The following MRCI calculations show that all configurations which contribute with an expansion factor of 0.1 or more to the CI wave function are considered as reference configurations.

The geometries used for all molecules were obtained from geometry optimizations of the electronic ground state at the B3LYP/6-31G* level using Gaussian98.³² The optimized S_1 geometry used in calculations on the molecules with four and five double bonds was obtained from CASSCF(8,8)/6-31G* (molecule **B**) and CASSCF(10,10)/6-31G* (molecule **C**) opti-

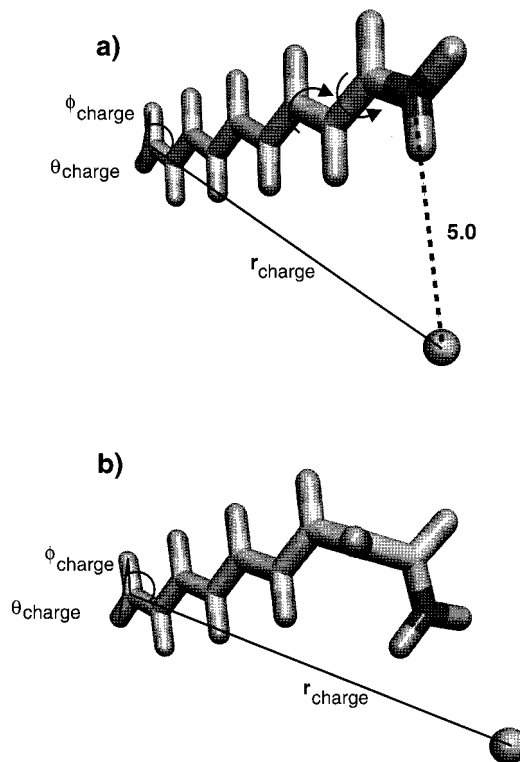


Figure 2. Definition of the position of the counterion and of the coordinate used for the double isomerization: (a) *all-trans* Schiff base with external charge at a distance of 5 Å from the nitrogen atom; (b) after rotation around bonds $C_{13}=C_{14}$ and $C_{14}=C_{15}$ by 90° .

mizations of the first excited state of both molecules by forcing the molecules to keep a planar structure. These geometry optimizations have been carried out with GAMESS.³³ The active space used for the CASSCF geometry optimizations of the S_1 states of both molecules has been chosen on the basis of MCSCF calculations using single and double excitations within a large active space. All important orbitals have been found to belong to symmetry a'' .

For modeling protein–chromophore interactions, we have placed a negative point charge at a distance of 5 Å from the nitrogen atom of the $=NH_2^+$ group of molecules **B** and **C**. The N–H axis approximately corresponds to the center of charge of the three counterions. Classical simulations have demonstrated that during enforced isomerization reactions of the retinal protonated Schiff base in bacteriorhodopsin, the positions of the counterion system consisting of Asp-85, Asp-212, and Arg-82 as well as the cyclohexene ring of the Schiff base are nearly kept fixed.^{34,35} We have therefore defined the position of this charge through the nonmoving part of the model molecules as shown in Figure 2 for molecule **C**. The parameters r_{charge} , ϕ_{charge} , and θ_{charge} have been chosen such that the distance between the nitrogen atom and the external negative charge is 5 Å in the *all-trans* conformation. The distance of 5 Å has been chosen in order to prevent unreasonably strong electrostatic interactions. Figure 2 also defines the coordinates used for the double isomerizations. The two torsions describing this isomerization are of opposite sign.

The chosen CASSCF/MRCI and HF/MRCI methods are computationally expensive. In particular we cannot afford to take structural relaxation into account. This shortcoming has several consequences. First, we can only determine crossings of electronic states by monitoring the character of the CI wave function. We can, however, not decide whether such a crossing corresponds to a conical intersection (i.e., a real crossing)^{36–38}

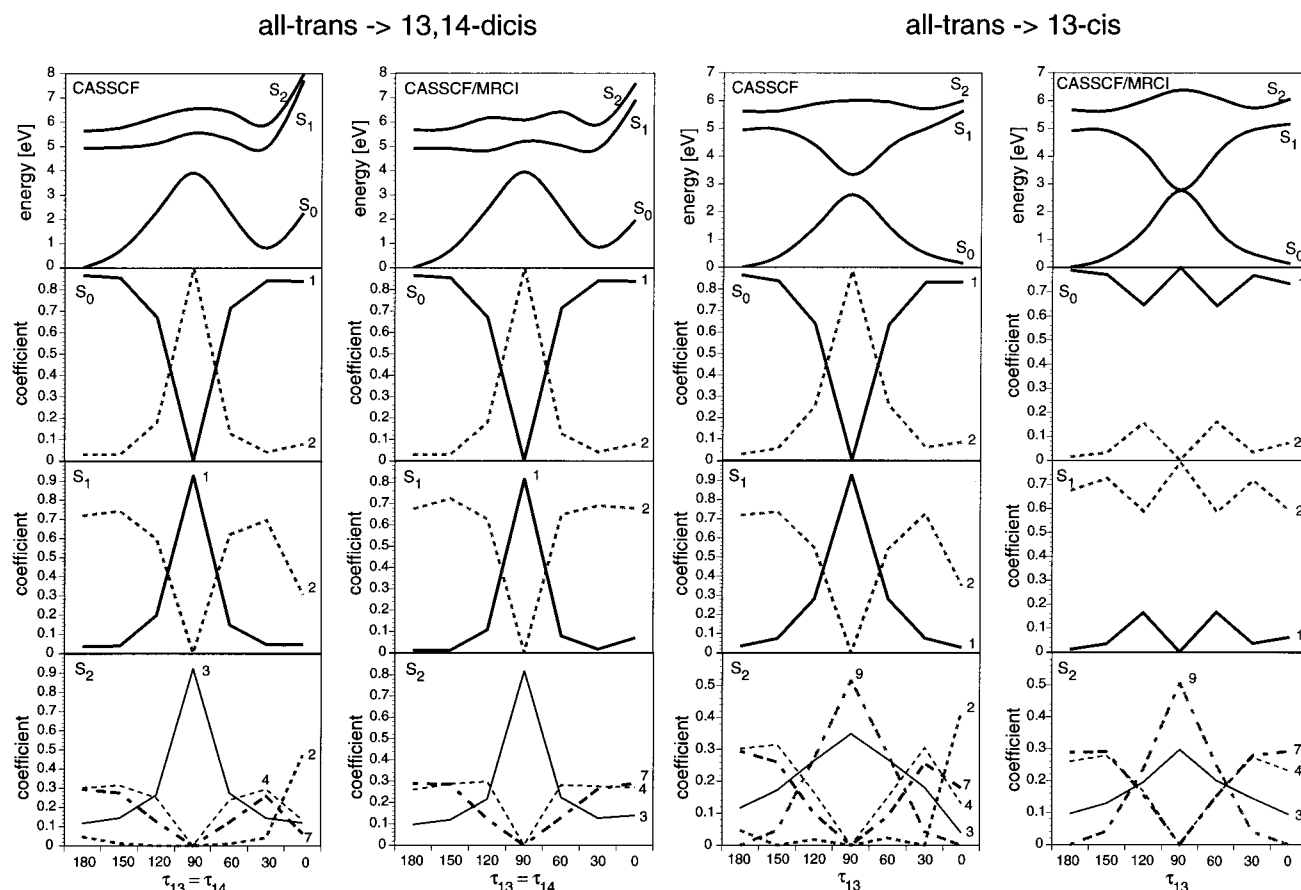


Figure 3. Potential energy profiles and CI expansion coefficients for *all-trans* \rightarrow 13,14-di-*cis* and *all-trans* \rightarrow 13-*cis* isomerizations of a protonated Schiff base model molecule with three conjugated double bonds calculated with the 6-31G* basis set.

or to an avoided crossing. Both situations should, however, allow a fast relaxation into the electronic ground state. Comparison of our results on molecule **A** with the results of Garavelli et al.^{38,12} suggests that their conical intersection corresponds to our S_0/S_1 crossing. Although a conical intersection is defined by energetical criteria, it has been stated that along an adiabatic potential surface the character of the wave functions changes appreciably in the vicinity of a conical intersection.³⁹ Second, since we cannot calculate reaction pathways but only nonrelaxed potential energy profiles, calculated barriers are always overestimated.

3. Results and Discussion

3.1. Molecule **A** with Three Conjugated Double Bonds: Comparison of CASSCF and CASSCF/MRCI Calculations.

Figure 3 shows energy profiles and CI coefficients for the isomerizations *all-trans* \rightarrow 13,14-di-*cis* and *all-trans* \rightarrow 13-*cis* calculated at the CASSCF and CASSCF/MRCI levels of theory using the 6-31G* basis set. From Figure 3 it is clear that only two configurations are important for the two isomerization reactions upon excitation into the first excited state S_1 : the first one is configuration **1** which corresponds to the electronic ground state and can be denoted as $(21)^2(22)^2$, and the second configuration is configuration **2** which corresponds to the singly excited configuration $(21)^2(22)^1(23)^1$. Figure 3 demonstrates that at the CASSCF level of theory crossing between the states S_1 and S_0 are predicted for both isomerization reactions. The result for the single isomerization thus agrees with the results of Schulten and co-workers^{15,16} and suggests that the found crossing corresponds to the conical intersection found by Garavelli et al.^{11,12} for this reaction coordinate. At the CASSCF/

MRCI level we find a crossing of the potential energy surfaces of the states S_0 and S_1 only in the case of the *all-trans* \rightarrow 13,14-di-*cis* reaction, while the crossing along the reaction coordinate of the single isomerization which has been predicted at the CASSCF level disappears. Since along this adiabatic potential profile no significant changes of the character of the wave functions are found,³⁹ we conclude that the conical intersection was most likely lost at this level of theory although the two states are nearly degenerate at a rotation angle of 90°.

The predictions provided by the CASSCF/MRCI calculations thus agree basically with those we have found with our previous HF/MRCI calculations.¹⁴ While the electronic structure of the states S_0 and S_1 is shown to be dominated by configurations **1** and **2**, the structure of state S_2 is more complicated. Many configurations are considerably contributing to its wave function. Among them, configuration **3**, which is denoted as $(21)^2(22)^1(24)^1$ and which thus corresponds to an excitation from the HOMO to the second lowest unoccupied orbital, becomes dominant during the double isomerization, and configuration **9**, which is denoted as $(21)^1(22)^1(23)^2$ and thus corresponds to a double excitation from the two highest occupied orbitals into the LUMO, becomes dominant during the single isomerization.

We assume that the crossing for the *all-trans* \rightarrow 13-*cis* single isomerization found at the CASSCF level is most likely an artifact caused by the state-averaging procedure. While the different quantum chemical methods differ in their prediction of crossings of electronic states, they agree quite well in their prediction of the shape of the energy profiles. None of the calculations predict a steep gradient in the Franck–Condon region which could explain a fast *all-trans* \rightarrow 13-*cis* process.

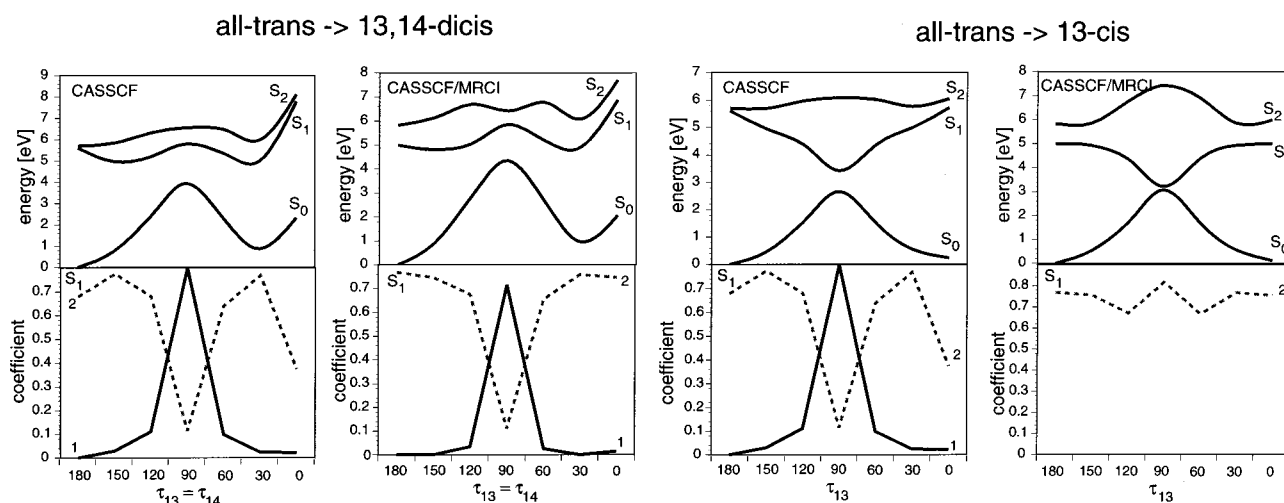


Figure 4. Potential energy profiles and CI expansion coefficients for *all-trans* \rightarrow 13,14-di-*cis* and *all-trans* \rightarrow 13-*cis* isomerizations of a protonated Schiff base model molecule with three conjugated double bonds calculated with the smaller 6-31G basis set.

In contrast, for both isomerization reactions, small barriers are predicted by the calculations. As stated in section 2, barriers are calculated using nonrelaxed structural parameters and are, thus, generally overestimated. Garavelli et al.^{11,12} have demonstrated that relaxations of bonds are very fast and occur most likely before an *all-trans* \rightarrow 13-*cis* isomerization reaction begins to develop. At the CASSCF/MRCI level of theory, consideration of geometry relaxation is unfortunately too expensive. We will, however, demonstrate in section 3.2 by using a CASSCF optimized excited-state geometry that relaxation of bond lengths and bond angles in the excited state indeed removes the barrier for an *all-trans* \rightarrow 13-*cis* single isomerization in the S_1 state. As noted before, during an isomerization reaction from the *all-trans* conformation to either 13,14-di-*cis* or 13-*cis*, the CI wave functions of the states S_0 and S_1 are dominated by the two configurations **1** and **2**. No significant contribution of a third configuration is found which could imply a crossing of the states S_1 and S_2 .

The results presented above are the results of large CASSCF/MRCI calculations. As noted in section 2 the dimension of the CI matrix in these calculations was nearly 8 million. We consider these calculations as our reference calculations for demonstrating that the predictions provided by state-averaged CASSCF and state-averaged CASSCF/MRCI calculations are different. The results moreover suggest that there is a good agreement between the predictions provided by the expensive CASSCF/MRCI calculation and those provided by the simpler HF/MRCI method. We will however demonstrate in a following section that this suggestion is only valid for a protonated Schiff base in vacuum. As soon as protein–chromophore interactions are taken into account, the two methods provide different predictions.

We have also carried out the same set of calculations using the smaller 6-31G basis set and a smaller CI expansion. Potential energy profiles and dominating configurations of the first excited state are shown in Figure 4. Qualitatively, the results correspond well to those of the ‘reference calculation’ discussed above. In particular, along the reaction coordinate of the single isomerization, a state crossing is found at the CASSCF level of theory but not at the CASSCF/MRCI level of theory. The finding that the consideration of polarization functions does not change the results significantly has already been mentioned by Schulten and co-workers¹⁶ and lets us believe that our calculations on the larger model molecules, where the inclusion of polarization

functions at this level of theory would be very expensive, are physically adequate. We have however to note that this smaller basis set seems to underestimate barriers in the vicinity of the *all-trans* structure. In particular, at the CASSCF level, a barrierless beginning of the two isomerization reactions is predicted.

From the calculations using the 6-31G* basis set we find the following transition energies: $S_0 \rightarrow S_1$, 4.91 eV (CASSCF/MRCI) and 4.94 eV (CASSCF); $S_0 \rightarrow S_2$, 5.67 eV (CASSCF/MRCI) and 5.63 eV (CASSCF). Surprisingly, the predicted $S_0 \rightarrow S_1$ transition energies are basically the same at the CASSCF and CASSCF/MRCI levels. Two factors are probably responsible for this finding: first, the state-averaged CASSCF method has been applied, and second, 28 virtual orbitals were frozen in the CI calculation. Optimizing the CASSCF wave function for each state separately leads to a transition energy of 5.00 eV. Following MRCI calculations for both states without freezing any virtual orbitals reduces this transition energy to 4.5 eV.⁴⁰ This value compares well with recent results of excited-state calculations using the ab initio effective Hamiltonian theory.⁴¹ Ab initio calculations at the CASSCF/MP2 level of theory using the MCQDPT2 method of Nakano as implemented in GAMESS,^{42,43} however, lets us suspect that the $S_0 \rightarrow S_1$ transition energy is still overestimated by 0.5–0.7 eV.⁴⁰

3.2. Molecule B with Four Conjugated Double Bonds: Effect of Protein–Chromophore Interaction and Geometry Relaxation. Potential energy profiles and CI coefficients for the model molecule with four conjugated double bonds calculated at the CASSCF/MRCI level of theory using the 6-31G basis set are depicted in Figure 5. For the *all-trans* \rightarrow 13,14-di-*cis* isomerization, we find again a crossing of the energy surfaces of the states S_0 and S_1 . During this isomerization the wave function of the first excited state S_1 is dominated by two configurations: that of the ground state, denoted as $(32)^2 (33)^2$, and that of a single HOMO \rightarrow LUMO excitation, denoted as $(32)^2 (33)^1 (34)^1$. For the isomerization *all-trans* \rightarrow 13-*cis* we also find a crossing of the S_1 state, however, not with the ground state but with a state which can be described by $(31)^2 (32)^1 (33)^2 (34)^1$ which corresponds to an excitation from the second highest occupied orbital into the lowest virtual orbital, a configuration which, according to the calculation of the *all-trans* conformer, contributes dominantly to the wave function of the second excited state. We thus find and S_0/S_1 crossing for the *all-trans* \rightarrow 13,14-di-*cis* isomerization and an S_1/S_2 crossing

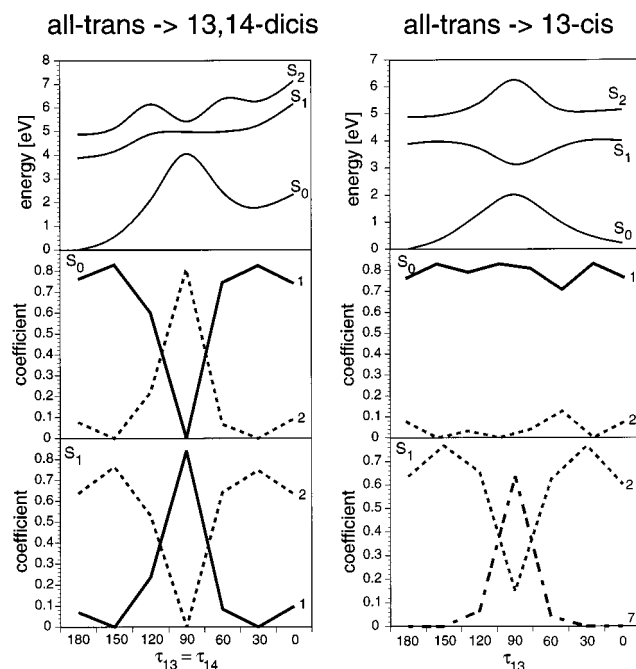


Figure 5. Potential energy profiles and CI expansion coefficients for *all-trans* \rightarrow 13,14-di-*cis* and *all-trans* \rightarrow 13-*cis* isomerizations of a protonated Schiff base model molecule with four conjugated double bonds.

for the *all-trans* \rightarrow 13-*cis* isomerization. This latter crossing is, however, not followed by a crossing of S_1 and the ground state and, therefore, does not offer a decay channel into the ground state. According to this calculation, a fast relaxation to the ground state should only occur along the reaction coordinate of the double isomerization. Although the barrier of about 8900 cm^{-1} is overestimated as previously discussed, the process most likely exhibits a nonvanishing barrier and is, therefore, not spontaneous.

How are potential energy profiles and contributing configurations to the wave functions affected when a counterion is added to the system? According to Figure 6 electrostatic interaction with the counterion causes now an S_0/S_1 crossing also for the *all-trans* \rightarrow 13-*cis* single isomerization. While the double isomerization still exhibits a barrier of $\sim 7000 \text{ cm}^{-1}$ which prevents a fast isomerization reaction, the rotation around the single bond is nearly barrierless and offers an efficient channel for a relaxation into the electronic ground state. To check for the effect of bond relaxation in the first excited state, we have redone this set of calculations by using a CASSCF(6,6)/6-31G* optimized structure of the S_1 state. Bond lengths of C–C and C–N bonds in the states S_0 and S_1 are listed in Table 1. The largest effects are found for bonds $C_{13}=C_{14}$ and $C_{11}=C_{12}$ which are 0.108 and 0.094 Å longer in the excited state than in the ground state. These bonds are thus considerably weakened and, therefore, allow a barrierless rotation in the excited state. The comparison of the energy profiles of the two systems in the vicinity of the *all-trans* structure is shown in Figure 7. The structural relaxation completely removes the small barrier for the single isomerization around the double bond $C_{13}=C_{14}$ while the energy still raises for the double isomerization.

Our calculations of this system demonstrate that protein–chromophore interactions make an efficient relaxation into the electronic ground state during an *all-trans* \rightarrow 13-*cis* single isomerization possible. After an initial fast relaxation of bond lengths this single isomerization is a barrierless process. This requested fast relaxation of bond lengths has previously been

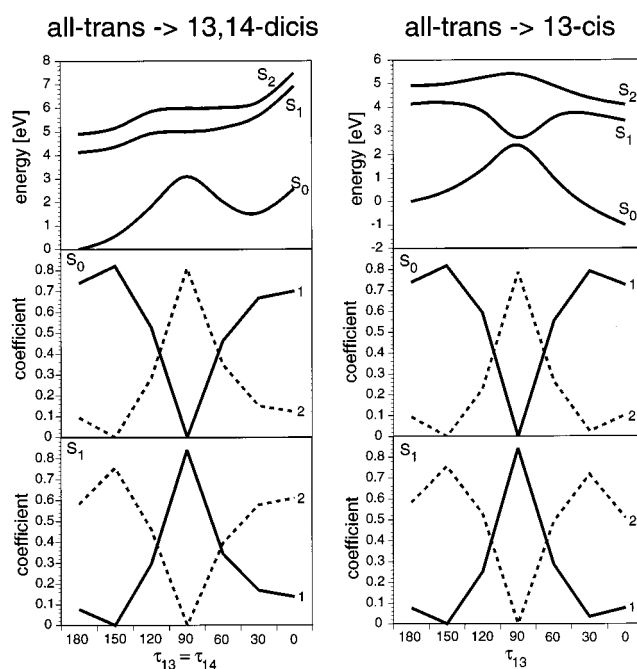


Figure 6. Potential energy profiles and CI expansion coefficients for *all-trans* \rightarrow 13,14-di-*cis* and *all-trans* \rightarrow 13-*cis* isomerizations of a protonated Schiff base model molecule with four conjugated double bonds and a negatively charged counterion. The ground-state geometry was used in this set of calculations.

TABLE 1: Optimized Bond Lengths (Å) in the States S_0 and S_1 of Molecules B and C

bond	molecule B			molecule C		
	S_0	S_1	Δ	S_0	S_1	Δ
$C_{15}-N$	1.3247	1.3458	0.021	1.3269	1.3365	0.010
$C_{14}-C_{15}$	1.3950	1.3754	-0.020	1.3915	1.3796	-0.012
$C_{13}-C_{14}$	1.3962	1.5042	0.108	1.3912	1.4594	0.068
$C_{12}-C_{13}$	1.4296	1.3578	-0.072	1.4029	1.3545	-0.048
$C_{11}-C_{12}$	1.3695	1.4634	0.094	1.3827	1.4767	0.094
$C_{10}-C_{11}$	1.4364	1.3867	-0.050	1.4152	1.3599	-0.055
C_9-C_{10}	1.3496	1.3905	0.041	1.3709	1.4362	0.065

proposed by Garavelli et al.^{11,12} on the basis of state-averaged CASSCF calculations and has been suggested from experiments with $C_{13}=C_{14}$ locked retinal analogues.²⁵

The calculated energy differences of the *all-trans* conformation are 3.88 eV ($S_0 \rightarrow S_1$) and 1.00 eV ($S_1 \rightarrow S_2$). From the results of CASSCF/MP2 ab initio calculations we assume that this energy of the $S_0 \rightarrow S_1$ transition is most likely overestimated by about 1 eV.⁴⁰ Upon addition of the counterion, the energy of the S_1 raises to 4.87 eV. This agrees qualitatively with the experimentally known blue shift of the chromophore due to interactions of the protonated Schiff base with counterions in solution or in the protein. The energy difference between the states S_1 and S_2 , on the other hand, is reduced to 0.72 eV which qualitatively agrees with the findings of Yamamoto et al.^{22,23}

3.3. Making the Conjugated System Longer: CASSCF/MRCI and HF/MRCI Calculations of a Molecule with Five Conjugated Double Bonds. The question arises of how far the length of the conjugated system might affect the results we have presented in sections 3.1 and 3.2. We have therefore additionally carried out HF/MRCI and CASSCF/MRCI calculations on a system with five conjugated double bonds, molecule C in Figure 1. We have carried out two sets of calculations on this molecule: one set consists of HF/MRCI and CASSCF/MRCI calculations on the free protonated Schiff base, i.e., the Schiff base without a counterion using the geometry of the ground

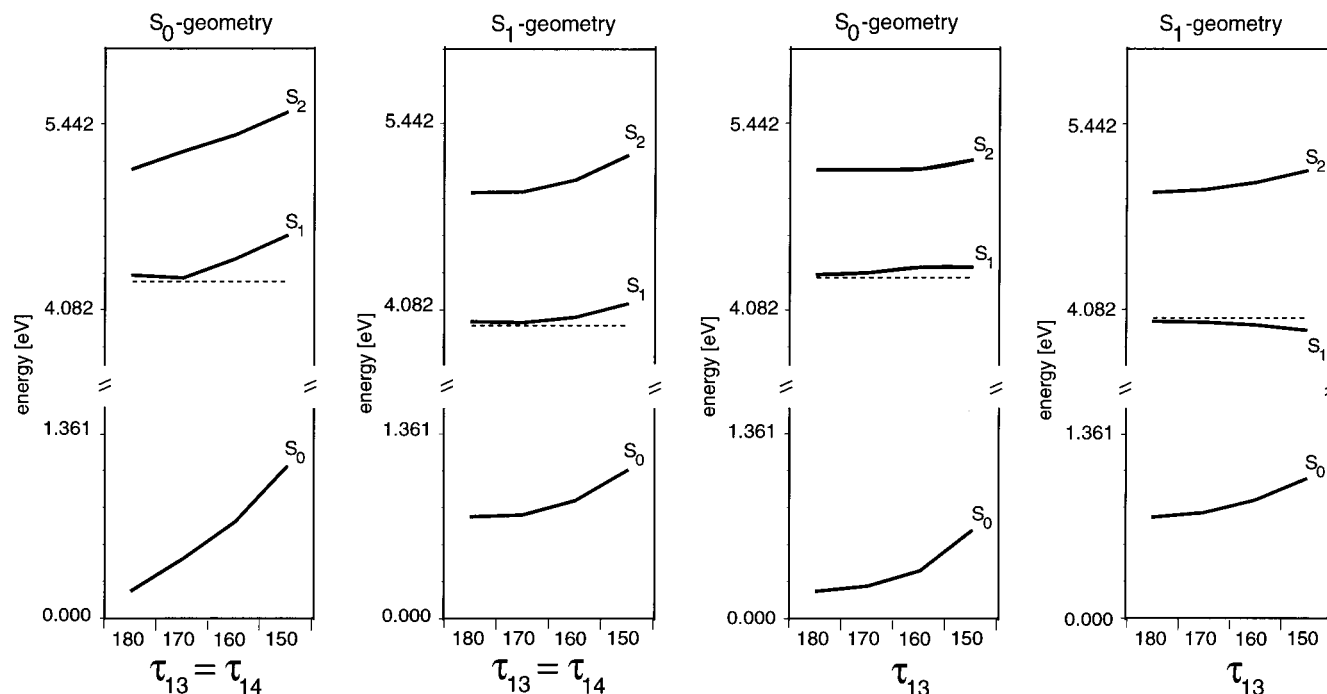


Figure 7. Comparison of potential energy profiles for the system with four conjugated double bonds and a counterion for S_0 and S_1 geometries for both isomerization models.

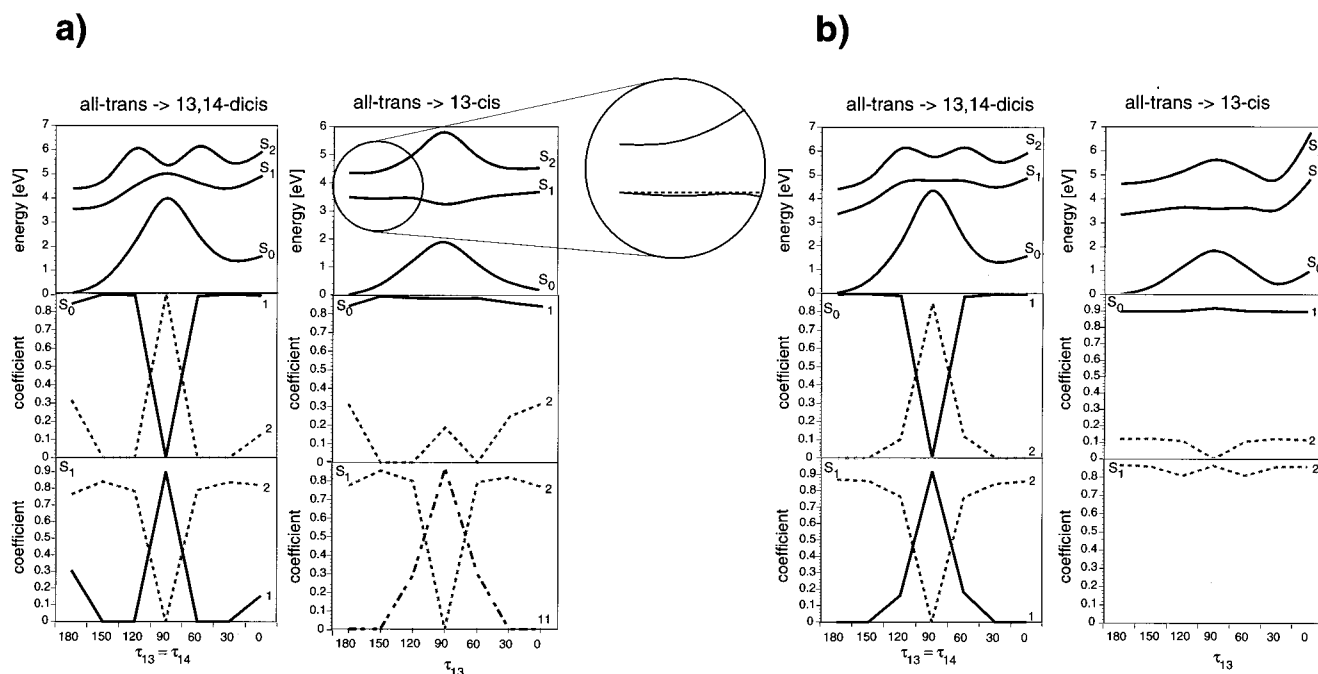


Figure 8. Potential energy profiles and CI expansion coefficients for *all-trans* \rightarrow 13,14-di-cis and *all-trans* \rightarrow 13-cis isomerizations of a protonated Schiff base model molecule with five conjugated double bonds. The ground-state geometry was used in these calculations: (a) CASSCF(6,6)/MRCI calculation; (b) HF/MRCI calculation.

state. The second set consists of HF/MRCI and CASSCF/MRCI calculations of the protonated Schiff base with an added counterion using the optimized structure of the excited state S_1 .

Figure 8 presents potential energy profiles and dominant configurations of the first set of calculations. The results of the CASSCF/MRCI (Figure 8a) and HF/MRCI (Figure 8b) calculations give basically the same predictions. For the double isomerization, the states S_0 and S_1 are clearly dominated by the two configurations 1 and 2. Configuration 1 corresponds to the Hartree–Fock determinant $((35)^2 (36)^2)$, and configuration 2

corresponds in good approximation to a single HOMO \rightarrow LUMO excitation $((35)^2 (36)^1 (37)^1)$. In the CASSCF/MRCI calculation of the single isomerization, we find a crossing of the S_1 with a state which corresponds to a double excitation from the HF determinant and is described by $(35)^2 (37)^2$. This configuration dominantly contributes to the wave function of the second excited state S_2 in the *all-trans* conformation. We find thus a perfect agreement with the results of molecule **B**: an S_0/S_1 crossing is found for the double isomerization and an S_1/S_2 crossing which is not connected to an S_0/S_1 crossing is found for the single isomerization. In agreement with our

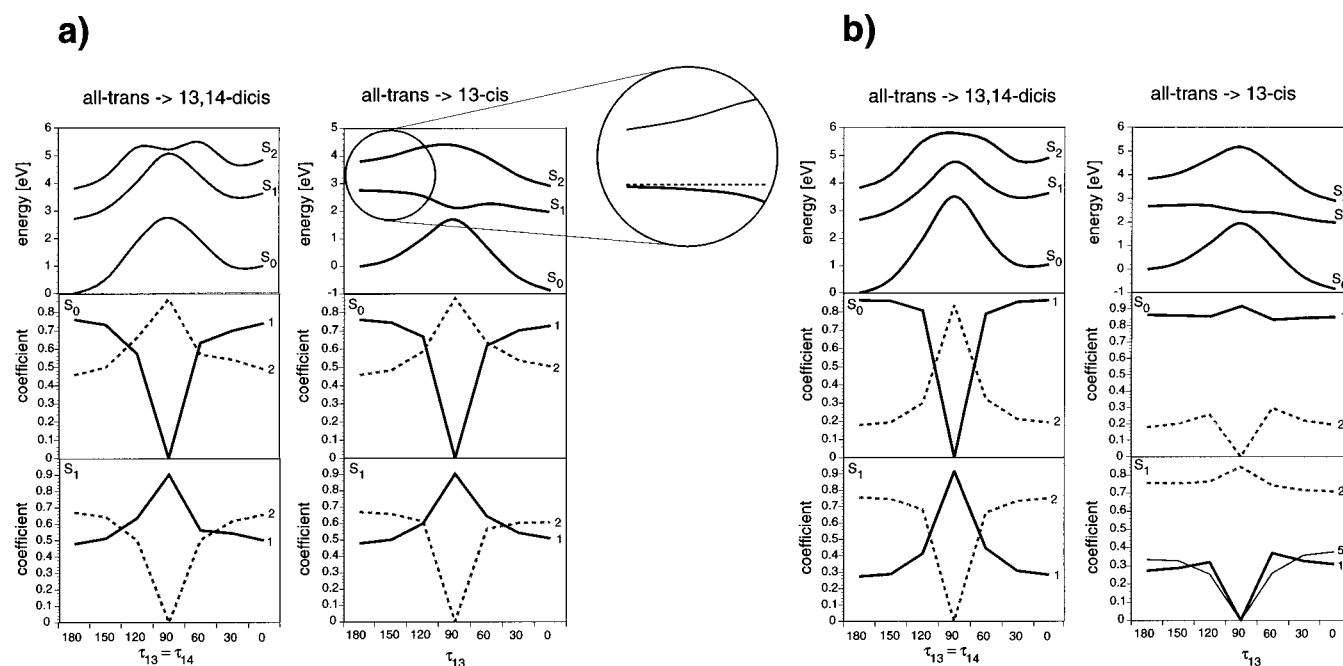


Figure 9. Potential energy profiles and CI expansion coefficients for *all-trans* \rightarrow 13,14-di-*cis* and *all-trans* \rightarrow 13-*cis* isomerizations of a protonated Schiff base model molecule with five conjugated double bonds. The geometry of the S_1 state was used in these calculations and a counterion was added: (a) CASSCF(6,6)/MRCI calculation; (b) HF/MRCI calculation.

calculations of smaller model molecules without a counterion, the HF/MRCI calculations predict a crossing of the states S_0 and S_1 only for the double isomerization *all-trans* \rightarrow 13,14-di-*cis*.

Figure 9 presents the potential energy profiles and important configurations of the second set of calculations. Again, panel a presents the results of the CASSCF/MRCI calculations and panel b those of the HF/MRCI calculations. The CASSCF/MRCI results agree well with our findings on the system with four conjugated double bonds presented in section 3.2: addition of a counterion causes an S_0/S_1 crossing along the reaction coordinate of the single isomerization *all-trans* \rightarrow 13-*cis*. Furthermore, addition of the counterion and structural relaxation in the excited state S_1 remove the barrier along this reaction coordinate and allow a fast relaxation into the electronic ground state. The comparison of the calculated bond lengths in the states S_0 and S_1 are given in Table 1. A significant elongation is found for bonds $C_{13}=C_{14}$ (0.068 Å) and $C_{11}=C_{12}$ (0.094 Å) which facilitates isomerization reactions around those bonds. The double isomerization, on the other hand, is connected with a high barrier of about 2.3 eV. Structural relaxation along both reaction coordinates would affect the energy profiles of both isomerization reactions. Compared to the ground-state geometry, the structure of the optimized planar S_1 state shows bond lengths for the $C_{13}-C_{14}$ and $C_{14}-C_{15}$ bonds which correspond closely to a single and double bond, respectively. We can assume that the double isomerization can most easily occur when the two involved bonds correspond to single bonds. We have calculated the energies of the point $\tau_{13} = \tau_{14} = 90^\circ$ using bond lengths of 1.45 Å for these two bonds, and we find that the barrier in the first excited state is reduced by not more than 0.2 eV. We can thus conclude that also upon structural relaxation, the single isomerization will still be clearly favored compared to the double isomerization. The calculations moreover suggest that in longer conjugated systems the bond $C_{11}=C_{12}$ is more elongated in the excited state than the bond $C_{13}=C_{14}$. This result might be one reason for the faster S_1 decay time of rhodopsin⁴⁴ compared to bacteriorhodopsin^{8,7} or halorhodopsin.⁴⁵

The results of the HF/MRCI calculations presented in Figure 9b provide predictions which disagree with those of the CASSCF/MRCI calculations. Here, the interaction with a counterion does not cause a crossing of the states S_0 and S_1 along the reaction coordinate of the single isomerization. The barrier for the single isomerization nearly vanishes. The barrier found for the double isomerization, however, is as high as 2.1 eV and makes a spontaneous decay into the ground state unlikely. The results of the HF/MRCI calculations are thus most likely not compatible with experimental findings.

4. Conclusions

Several important conclusions can be drawn from the presented calculations. From the methodological point of view, we have demonstrated that for a free protonated Schiff base, HF/MRCI and CASSCF/MRCI methods give qualitatively similar predictions. Both methods predict an S_0/S_1 crossing only along the reaction coordinate of a double isomerization *all-trans* \rightarrow 13,14-di-*cis*. These predictions disagree with those provided by state-averaged CASSCF calculations where such a crossing of ground state and excited state is also predicted for the *all-trans* \rightarrow 13-*cis* single isomerization. We suggest that these latter findings are an error caused by the procedure of state averaging. This state averaging, however, is necessary in order to ensure convergence in the CASSCF calculations. The MRCI calculations we have performed on top of the state-averaged CASSCF calculations in our study can most likely correct for this error.

When protein–chromophore interactions are modeled by adding a counterion to the protonated Schiff base, the predictions provided by HF/MRCI and CASSCF/MRCI calculations are different. While the counterion seems to affect the results of the HF/MRCI calculations only weakly, the wave functions of the CASSCF/MRCI calculations are considerably affected. Most important, the addition of a counterion causes at this level of theory an S_0/S_1 crossing also along the reaction coordinate of the *all-trans* \rightarrow 13-*cis* single isomerization. Furthermore, after

a preceding fast relaxation of bond lengths in the excited state S_1 the barrier for this single isomerization is completely removed. The calculations at the CASSCF/MRCI level of theory can thus provide predictions which agree with experimental data and which can explain how the fast decay into the electronic ground state during an *all-trans* \rightarrow *cis* isomerization of the chromophore could be achieved. The findings of our investigation show that the level of theory used for quantum chemical calculations of such systems must be chosen very carefully. It is in particular necessary to account at a proper level for dynamic correlation effects by means of a large MRCI expansion as well as for static correlation effects by taking a CASSCF wave function as the reference wave function for the configuration interaction procedure.

How does our study affect the discussion of the primary reaction of bacteriorhodopsin? Among the huge amount of available spectroscopic data of this protein, two relaxation times are of special interest in the context of the present investigation. After light excitation of the protein, a fast first relaxation time of about 200 fs has been found.⁸ An even faster primary relaxation process which occurs within less than 30 fs has recently been found in experiments using retinal as well as $C_{13}=C_{14}$ locked retinal analogues.²⁵ A similar fast first relaxation time is also found for the chlorine pump halorhodopsin⁴⁵ which has a similar structure to bacteriorhodopsin but lacks the negatively charged residue Asp-85 in the vicinity of the protonated Schiff base and for the protonated retinal Schiff base in solution.^{46,47} This very fast first relaxation time is thus nearly independent of the environment. From the experiments with locked retinal analogues and from the results of the calculations of Garavelli et al.,^{11,12} it can be concluded that this process is not connected with any torsional motion but corresponds to a very fast relaxation of bond lengths in the excited state. In agreement with these findings, our calculations show that such a relaxation is necessary in order to provide a barrierless reaction path toward the region of the S_0/S_1 crossing. This is necessary for making a fast relaxation into the electronic ground state possible.

The second time constant which corresponds to the relaxation into the electronic ground state and which is connected with the isomerization reaction, however, varies strongly in different systems. In bacteriorhodopsin, this second process occurs within 500 fs^{7,8} while it is considerably slower in halorhodopsin⁴⁵ or in solution.^{46,47} This process which strongly depends on the environment could be affected through either steric or electrostatic interactions of the chromophore with the protein. Experiments on the excited-state dynamics of a protonated retinal Schiff base in solution⁴⁷ as well as the findings that the decay into the ground state is slowed considerably when Asp-85 is mutated into a neutral residue in bacteriorhodopsin^{48–50} suggest that this process is dominantly controlled by electrostatic interactions of the chromophore with its environment. This suggestion agrees with the findings of our present investigation. Electrostatic interactions not only affect the shape of the potential energy profiles but also affect the character of the wave functions of the electronic states. To provide an efficient primary step of the photocycle, electrostatic interaction with the environment is needed to induce a crossing between ground state and first excited state along the reaction coordinate of the *all-trans* \rightarrow 13-*cis* isomerization. Furthermore, a very fast relaxation of bond lengths in the excited state is needed to remove the barrier along this reaction coordinate. From our calculations we have also to conclude that the shape of the potential energy surface of the excited state most likely favors the *all-trans* \rightarrow 13-*cis*

single isomerization reaction. Furthermore, we cannot find any evidence in our calculations for a crossing of the potential energy surfaces of the states S_2 and S_1 along a reaction coordinate which leads to the region of the S_0/S_1 crossing. Such a pathway for the isomerization reactions has been previously suggested by Schulten and co-workers^{15,16} on the basis of CASSCF calculations. It might be interesting to note that such a crossing of the states S_2 and S_1 has indeed been found in polyenes.⁵¹ Garavelli et al. have however shown with their CASSCF calculations that the excited-state properties of polyenes and protonated Schiff bases are different.¹²

On the basis of our calculations we can postulate a mechanism for the fast photoisomerization reactions around $C=C$ double bonds as found in bacteriorhodopsin and in other retinal proteins such as halorhodopsin or rhodopsin. The catalytic effect of the protein environment is thus predicted to be dominantly of electrostatic nature. Electrostatic interactions with the protein cause a crossing between ground state and excited state along the barrierless isomerization coordinate and allow a fast relaxation into the electronic ground state. Spectroscopic data of different retinal proteins^{8,7,45} and in particular of mutated retinal proteins^{48–50} show that the electronic structure of the chromophore and, thereby, its behavior after light excitation is very sensitive to changes of the external electric field. A proper arrangement of external charges is necessary in order to make an efficient decay into the ground state possible. The structures of the wild type proteins are most likely optimized for accelerating the isomerization reactions involved in the photocycle.

Our model of chromophore–counterion interaction is too simple to be able to predict such details. A deeper insight into these mechanisms could be expected from QM/MM hybrid simulations. Such calculations have in the past mostly been performed using semiempirical^{52,53} or density functional^{54–60} methods for the description of the quantum mechanical part of the system. In the case of bacteriorhodopsin we must deal with the electronically excited state. Moreover, we have demonstrated in this contribution that quantum chemical calculations at a rather high level of theory seem to be necessary for a physically accurate description of this class of molecules. Such type of calculations are most likely not feasible with the currently available computational techniques and computer hardware even for model molecules of the retinal chromophore.

Acknowledgment. The author thanks Wolfgang Zinth and Paul Tavan for many valuable discussions. Financial support by the Volkswagen Stiftung (Project I/73 224) is gratefully acknowledged.

References and Notes

- (1) Ottolenghi, M.; Sheves, M. *Isr. J. Chem.* **1995**, *35*, 193.
- (2) Haupts, U.; Tittor, J.; Oesterhelt, D. *Annu. Rev. Biophys. Biomol. Struct.* **1999**, *28*, 367–399.
- (3) Fodor, S. P. A.; Ames, J. B.; Gebhard, R.; van den Berg, E. M. M.; Stoeckenius, W.; Lugtenburg, J.; Mathies, R. A. *Biochemistry* **1988**, *27*, 7097–7101.
- (4) Schulten, K.; Tavan, P. *Nature* **1978**, *272*, 85–86.
- (5) Schulten, K. In *Energetics and Structure of Halophilic Microorganisms*; Caplan, S.; Ginzburg, M., Eds.; Elsevier: Amsterdam, 1978; pp 331–334.
- (6) Gerwert, K.; Siebert, F. *EMBO J.* **1986**, *4*, 805–812.
- (7) Mathies, R. A.; Brito Cruz, C. H.; Pollard, W. T.; Shank, C. V. *Science* **1988**, *279*, 277–279.
- (8) Dobler, J.; Zinth, W.; Kaiser, W.; Oesterhelt, D. *Chem. Phys. Lett.* **1988**, *144*, 215–220.
- (9) Hasson, K. C.; Gai, F.; Anfinrud, P. A. *PNAS* **1996**, *93*, 15124–15129.

- (10) Gai, F.; Hasson, K. C.; McDonald, J. C.; Anfinrud, P. A. *Science* **1998**, 279, 1886–1891.
- (11) Garavelli, M.; Negri, F.; Olivucci, M. *J. Am. Chem. Soc.* **1999**, 121, 1023–1029.
- (12) Garavelli, M.; Bernardi, F.; Olivucci, M.; Vreven, T.; Klein, S.; Celani, P.; Robb, M. A. *Faraday Discuss.* **1998**, 110, 51–70.
- (13) Garavelli, M.; Bernardi, F.; Robb, M. A.; Olivucci, M. *J. Mol. Struct. (THEOCHEM)* **1999**, 463, 59–64.
- (14) Dobado, J. A.; Nonella, M. *J. Phys. Chem.* **1996**, 100, 18282–18288.
- (15) Schulten, K.; Humphrey, W.; Logunov, I.; Sheves, M.; Xu, D. *Isr. J. Chem.* **1995**, 35, 447–464.
- (16) Humphrey, W.; Lu, H.; Logunov, I.; Werner, H. J.; Schulten, K. *Biophys. J.* **1998**, 75, 1689–1699.
- (17) Schoenlein, R. W.; Peteanu, L. A.; Mathies, R. A.; Shank, C. V. *Science* **1991**, 254, 412–415.
- (18) Wang, Q.; Schoenlein, R. W.; Peteanu, L. A.; Mathies, R. A.; Shank, C. V. *Science* **1994**, 266, 422–424.
- (19) Kochendoerfer, G.; Mathies, R. A. *J. Phys. Chem.* **1996**, 100, 14526–14532.
- (20) Molteni, C.; Frank, I.; Parrinello, M. *J. Am. Chem. Soc.* **1999**, 121, 12177–12183.
- (21) Frank, I.; Hutter, J.; Marx, D.; Parrinello, M. *J. Chem. Phys.* **1998**, 108, 4060–4069.
- (22) Yamamoto, S.; Wasada, H.; Kakitani, K. *J. Mol. Struct. (THEOCHEM)* **1998**, 451, 151–162.
- (23) Yamamoto, S.; Wasada, H.; Kakitani, K. *J. Mol. Struct. (THEOCHEM)* **1999**, 462, 463–471.
- (24) Zhong, Q.; Ruhman, S.; Ottolenghi, M.; Sheves, M.; Friedman, N.; Atkinson, G. H.; Delaney, J. K. *J. Am. Chem. Soc.* **1996**, 118, 12828.
- (25) Ye, T.; Friedman, N.; Gat, Y.; Atkinson, G. H.; Sheves, M.; Ottolenghi, M.; Ruhman, S. *J. Phys. Chem. B* **1999**, 103, 5122–5130.
- (26) Lischka, H.; Shepard, R.; Shavitt, I.; Brown, F.; Pitzer, R.; Ahlrichs, R.; Böhm, H.-J.; Chang, A.; Comeau, D.; Gdanitz, R.; Dachsel, H.; Erhard, C.; Ernzerhof, M.; Höchtl, P.; Irle, S.; Kedziora, G.; Kovar, T.; Müller, T.; Parasuk, V.; Pepper, M.; Scharf, P.; Schiffer, H.; Schindler, M.; Schüler, M.; Szalay, P.; Zhao, J.-G. Columbus, an ab initio electronic structure program, release 5.3; 1997.
- (27) Shepard, R.; Shavitt, I.; Pitzer, R. M.; Comeau, D. C.; Pepper, M.; Lischka, H.; Szalay, P. G.; Ahlrichs, R.; Brown, F. B.; Zhao, J. G. *Int. J. Quant. Chem.* **1988**, 149.
- (28) Helgaker, T.; Jensen, H. J. A.; Jørgensen, P.; Olsen, J.; Ruud, K.; Ågren, H.; Andersen, T.; Bak, K. L.; Bakken, V.; Christiansen, O.; Dahle, P.; Dalskov, E. K.; B., T. E.; Fernandez, H.; Hetttema, H.; Jonsson, D.; Kirpekar, S.; Kobayashi, R.; Koch, H.; Mikkelsen, K. V.; Norman, P.; Packer, M. J.; Saue, T.; Taylor, P. R.; Vahtras, O. Dalton, release 1.0; April 1997.
- (29) Ditchfield, R.; Hehre, W. J.; Pople, J. A. *J. Chem. Phys.* **1971**, 54, 724.
- (30) Hehre, W. J.; Ditchfield, R.; Pople, J. A. *J. Chem. Phys.* **1972**, 56, 2257.
- (31) Franci, M. M.; Pietro, W. J.; Hehre, W. J.; Binkley, J. S.; Gordon, M. S.; DeFrees, D. J.; Pople, J. A. *J. Chem. Phys.* **1982**, 77, 3654.
- (32) Frisch, M. J.; Trucks, G. W.; Schlegel, H. B.; Scuseria, G. E.; Robb, M. A.; Cheeseman, J. R.; Zakrzewski, V. G.; Montgomery, J. A., Jr.; Stratmann, R. E.; Burant, J. C.; Dapprich, S.; Millam, J. M.; Daniels, A. D.; Kudin, K. N.; Strain, M. C.; Farkas, O.; Tomasi, J.; Barone, V.; Cossi, M.; Cammi, R.; Mennucci, B.; Pomelli, C.; Adamo, C.; Clifford, S.; Ochterski, J.; Petersson, G. A.; Ayala, P. Y.; Cui, Q.; Morokuma, K.; Malick, D. K.; Rabuck, A. D.; Raghavachari, K.; Foresman, J. B.; Cioslowski, J.; Ortiz, J. V.; Stefanov, B. B.; Liu, G.; Liashenko, A.; Piskorz, P.; Komaromi, I.; Gomperts, R.; Martin, R. L.; Fox, D. J.; Keith, T.; Al-Laham, M. A.; Peng, C. Y.; Nanayakkara, A.; Gonzalez, C.; Challacombe, M.; Gill, P. M. W.; Johnson, B.; Chen, W.; Wong, M. W.; Andres, J. L.; Gonzalez, C.; Head-Gordon, M.; Replogle, E. S.; Pople, J. A. Gaussian 98, revision a.7; Gaussian, Inc., Pittsburgh, PA; 1998.
- (33) Schmidt, M. W.; Baldridge, K. K.; Boatz, J. A.; Elbert, S. T.; Gordon, M. S.; Jensen, J. H.; Koseki, S.; Matsunaga, N.; Nguyen, K. A.; Su, S. J.; Windus, T. L.; Dupuis, M.; Montgomery, J. A. *J. Comput. Chem.* **1993**, 14, 1347–1363.
- (34) Nonella, M.; Windemuth, A.; Schulten, K. *Photochem. Photobiol.* **1991**, 54, 937–948.
- (35) Zhou, F.; Windemuth, A.; Schulten, K. *Biochemistry* **1993**, 32, 2291–2306.
- (36) Michl, J.; Bonacic-Koutecky, V., Eds. *Electronic Aspects of Organic Photochemistry*; Wiley: New York, 1990.
- (37) Klessinger, M. *Angew. Chem.* **1995**, 107, 597.
- (38) Garavelli, M.; Celani, P.; Bernardi, F.; Robb, M. A.; Olivucci, M. *J. Am. Chem. Soc.* **1997**, 119, 6891–6901.
- (39) Klessinger, M.; Michl, J. *Excited States and Photochemistry of Organic Molecules*; VCH: New York, 1995.
- (40) Nonella, M. Manuscript in preparation.
- (41) Martin, C. H.; Birge, R. R. *J. Phys. Chem. A* **1998**, 102, 852.
- (42) Nakano, H. *J. Chem. Phys.* **1993**, 99, 7983.
- (43) Nakano, H. *Chem. Phys. Lett.* **1993**, 207, 372.
- (44) Peteanu, L. A.; Schoenlein, R. W.; Wang, Q.; Mathies, R. A.; Shank, C. V. *Proc. Natl. Acad. Sci. U.S.A.* **1993**, 90, 11762.
- (45) Arlt, T.; Schmidt, S.; Zinth, W.; Haupts, U.; Oesterheld, D. *Chem. Phys. Lett.* **1995**, 241, 559–565.
- (46) Hamm, P.; Zurek, M.; Röscher, T.; Patzelt, H.; Oesterheld, D.; Zinth, W. *Chem. Phys. Lett.* **1996**, 263, 613–621.
- (47) Logunov, S. L.; Song, L.; El-Sayed, M. A. *J. Phys. Chem.* **1996**, 100, 18586–18591.
- (48) Song, L.; El-Sayed, M. A.; Lanyi, J. K. *Science* **1993**, 261, 891.
- (49) Logunov, S. L.; El-Sayed, M. A.; Song, L.; Lanyi, J. K. *J. Phys. Chem.* **1996**, 100, 2391–2398.
- (50) Zinth, W. Personal communication.
- (51) Hudson, B. S.; Kohler, B. E.; Schulten, K. In *Excited states*; Lim, E. C., Ed.; Academic Press: New York, 1982; p 1.
- (52) Bash, P. A.; Field, M. J.; Karplus, M. *J. Am. Chem. Soc.* **1987**, 109, 8092.
- (53) Field, M. J.; Bash, P. A.; Karplus, M. *J. Comput. Chem.* **1990**, 11, 700.
- (54) Stanton, R. V.; Hartsough, D. S.; Merz, K. M. *J. Phys. Chem.* **1993**, 97, 11868.
- (55) Svenssons, M.; Humbel, S.; Froese, R. D. J.; Matsubara, T.; Sieber, S.; Morokuma, K. *J. Phys. Chem.* **1996**, 100, 19357.
- (56) Matsubara, T.; Maseras, F.; Koga, N.; Morokuma, K. *J. Phys. Chem.* **1996**, 100, 2573.
- (57) Tunón, I.; Martins-Costa, M. T. C.; Millot, C.; Ruiz-López, M. F.; Rivail, J. L. *J. Comput. Chem.* **1996**, 17, 19.
- (58) Tunón, I.; Martins-Costa, M. T. C.; Millot, C.; Ruiz-López, M. F. *J. Chem. Phys.* **1997**, 106, 3633.
- (59) Strnad, M.; Martins-Costa, M. T. C.; Millot, C.; Tunón, I.; Ruiz-López, M. F.; Rivail, J. L. *J. Chem. Phys.* **1997**, 106, 3643.
- (60) Eichinger, M.; Tavan, P.; Hutter, J.; Parrinello, M. *J. Chem. Phys.* **1999**, 110, 10452.